Stretching an Elastic Loop: Crease, Helicoid, and Pop Out

Yasuaki Morigaki,[1] Hirofumi Wada,[2,*] and Yoshimi Tanaka[1,†]
[1]Graduate School of Environmental and Information Sciences, Yokohama National University, Yokohama 240-8501, Japan
[2]Department of Physics, Ritsumeikan University, Kusatsu, Shiga 525-8577, Japan
(Received 8 August 2016; published 3 November 2016)

Under geometric constraints, a thin structure can respond to an external loading in an unexpected way. A paper strip that is looped and pulled can be used for simple experimentation of such a process. Here, we study this seemingly very simple phenomenon in detail by combing experiments and theory. We identify the three types of shape transitions, i.e., crease, helicoid, and pop out, from a stretched loop, and classify them in terms of parameters characterizing a ribbon geometry. We establish a transition-type diagram by compiling our extensive experimental data. Numerical simulations based on the Kirchhoff rod theory and scaling argument reveal that the pop-out transition is governed by a single characteristic length $\xi \sim b^2/h$, where b and h are the ribbon's width and thickness, respectively. We also reveal the key roles of other physical effects such as the anisotropy of the bending elasticity and plastic deformations upon the shape selection mechanisms of a constraint ribbon.

DOI: 10.1103/PhysRevLett.117.198003

A loop under tension arises across different length scales. Examples include DNA filaments interacting with proteins in cell environments [1,2], nanobelts [3], gift-wrapping ribbons [4], knots in ties or shoelaces [5,6], wire clay or cheese cutters, surgical wires for ligation, and submarine cables [7]. The interplay between the geometry, topology, and elasticity as well as other physical effects determines the complex behaviors of such loops.

For a rod and wire, because the cross-sectional sizes are much smaller than the arclength, a one-dimensional (1D) description has been established and applied [8,9]. However, a ribbon, which is 1D-like at its arclength scale, can be viewed locally as two dimensional since its width and thickness are largely different. Thus, a ribbon geometry is often phrased as an intermediate between a rodlike (1D) and a sheetlike (2D) object [10]. Choosing a dimensional description one should apply to describe a ribbon is a difficult issue, and generally depends on a scale of description, boundary conditions, and geometric constraints [11–13]. At a length scale comparable to the ribbon's largest extent, an effective 1D elastic model has been established by considering the effects of in-plane stretch elasticity [14–18]. However, the questions of when the dimensional crossover occurs and how it influences the shape selection of a ribbon have still not been satisfactorily answered.

Here, we propose an experimental setup that allows the investigation of a ribbon's effective dimension by controlling a single parameter δ defined in Figs. 1(a) and 1(b). As the ribbon of width b and thickness h is pulled, different shape transitions, i.e., crease, helicoid, or pop out, from a tightened loop are observed depending on subtle control of the transverse distance δ. By performing systematic physical experiments, we classify the three types of transitions in terms of the parameters characterizing the ribbon geometry. Emphasis is then given to the pop-out elastic instability. To rationalize the observed behavior, we employ numerical and analytical approaches based on the Kirchhoff's elastic rod theory, and demonstrate the pivotal role of the characteristic length $\xi \sim b^2/h$.

Recent studies have shown that elastic helical ribbons can display stretching instabilities [19–22]. These studies

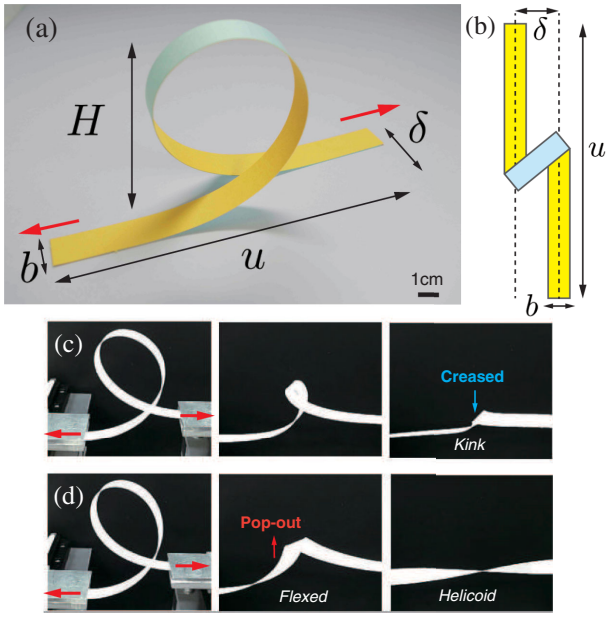

FIG. 1. (a),(b) Configuration of a looped ribbon and definition of the basic parameters, i.e., ribbon's width b, end-to-end distance u, gap distance between the centerline of the ribbon's ends δ, and height of ribbon's top H. (c),(d) Sequence of snapshots of a paper ribbon during the stretching process in experiments. (c) crease: $(L, b, \delta) = (212, 10, 30)$ mm; (d) pop out: $(L, b, \delta) = (212, 10, 35)$ mm.

distinctly differ from ours in two respects. First, our ribbon is intrinsically flat and does not possess any intrinsic curvatures. Second, neither end of our ribbon rotates about its axis (i.e., the linking number is conserved to unity), but helical ribbons in the previous studies were allowed to do so; otherwise, continuous unlooping was unattainable. At this point, we note an important contribution by Goss *et al.* [23], who reported experimental investigations of both the hockling and pop-out responses of a twisted rod under tension at $\delta = 0$ in our notation. Here, we will show that the δ dependence results in an entirely new physics in the ribbon mechanics, thereby generalizing the previous studies for looped rods and elastica [7,22–25].

A flat ribbon was cut out from a filter paper (Wattman, No. 1002-917, Wattman Co.) with a uniform thickness $h = 0.19$ mm. We carefully introduced a loop in the ribbon by hand and clamped both ends to set the transverse gap δ (see Fig. 1). We stretched the ribbon at a constant pulling speed while keeping δ fixed, and recorded the subsequent shape changes in a video. The morphologies of the ribbon were then analyzed by capturing the images from those videos. The geometric quantities characterizing a ribbon configuration are the arclength L, width b, and δ, which we varied in the range 112–262 mm, 1–12 mm, and 5–65 mm, respectively, in the experiments. Hereafter, we represent these as a triplet number (L, b, δ) in the unit of [mm]. The stretching speed ranges from 2 to 20 mm/s, corresponding to a quasistatic stretching where the overall shape dynamics is insensitive to the speed (except in the very vicinity of the transition points). A fresh paper ribbon was used for each experiment.

Figures 1(c) and 1(d) show the behavior of the ribbon during the stretching process for $(L, b, \delta) = (212, 10, 30)$ and (212,10,35). As the ribbon is stretched, the loop gets progressively smaller. When the loop becomes sufficiently small, a further stretching triggers two qualitatively different shape dynamics depending on δ. For small δ, the loop creases to form a kink [Fig. 1(c)], and the ribbon tears off before it is stretched out. The collapse of the loop is characterized by plastic deformations at the singularity region [26]. In contrast, when δ is larger, the tightened loop suddenly opens, culminating in a helicoidal shape when it is stretched out [Fig. 1(d)]. The ribbon seems to respond almost elastically during this entire process.

For fixed L and b, we can find a critical gap distance $\delta_{CP} = \delta_{CP}(L, b)$, below which ($\delta < \delta_{CP}$) a ribbon creases, and above which ($\delta > \delta_{CP}$) the ribbon "pops out." The transition is subtle; close to δ_{CP}, a ribbon's behavior depends strongly on experimental uncertainties. To statistically address this, we repeated ten independent experiments for each δ, and the probability of the pop-out event $p(\delta)$ has been constructed [27]. We found that $p(\delta)$ rapidly increases as δ crosses δ_{CP}. The value of δ_{CP} was then determined from the condition $p(\delta_{CP}) \sim 0.5$. Therefore, we needed to perform several tens of experiments to determine

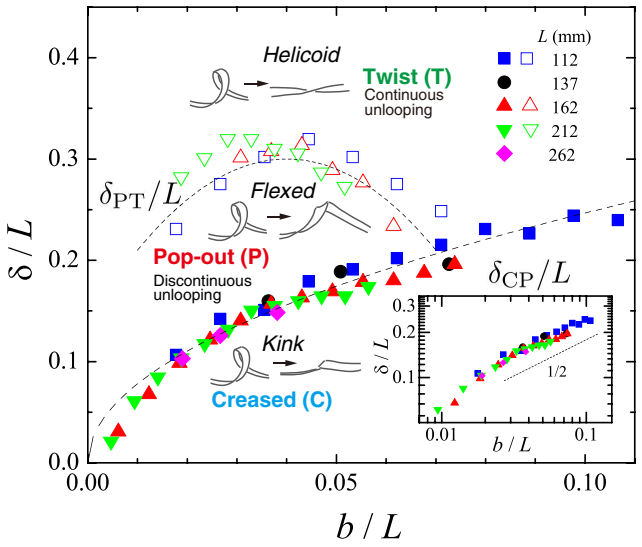

FIG. 2. Transition-type diagram in the stretching process for a looped paper ribbon, drawn on the $(b/L, \delta/L)$ parameter space. Symbols are data from our δ-controlled experiments for different lengths L and widths b. δ_{CP} and δ_{PT} represent the boundaries between creased (C) and pop out (P), and between pop out and twist (T) transitions, respectively. The inset is a log-log plot of the same data of δ_{CP}, suggesting data collapse with power law of exponent $1/2$.

one point plotted in Fig. 2, which amounts to a few thousand experiments in total to construct the whole diagram. When δ_{CP} are plotted in the form of δ_{CP}/L vs b/L, they compose a single master curve, defining the boundary separating the crease (C) and pop out (P) transition regimes [Fig. 2]. Further, a log-log plot of the same data (inset in Fig. 2) suggests

$$\delta_{CP} \sim (bL)^{1/2}. \tag{1}$$

A precise physical interpretation of Eq. (1) will be a theoretical challenge in future studies. Importantly, the scaling relation in Eq. (1) may provide a simple and practical guideline for the operation of ribbonlike structures without causing any permanent damages.

Depending on (b, L, δ), unlooping occurs via either discontinuous or continuous shape changes. The pop out is apparently discontinuous. The ribbon's top suddenly jumps up so that the ribbon takes its characteristic flexed configuration [Fig. 3(a)]. In contrast, for sufficiently large δ, a loop transits continuously to a helicoidal shape. This transition is similar to the spontaneous spiral-to-helicoid transition studied previously [29,30]. The distinction between these two morphologies is based on the shape of the ribbon's centerline. The "flexed" shape has a localized curvature at its middle, while the "helicoid" has an approximately straight centerline. For a given parameter set of (L, b), a critical gap distance δ_{PT} between these two was experimentally determined in the same way as δ_{CP}, and is plotted in Fig. 2. While the data for different

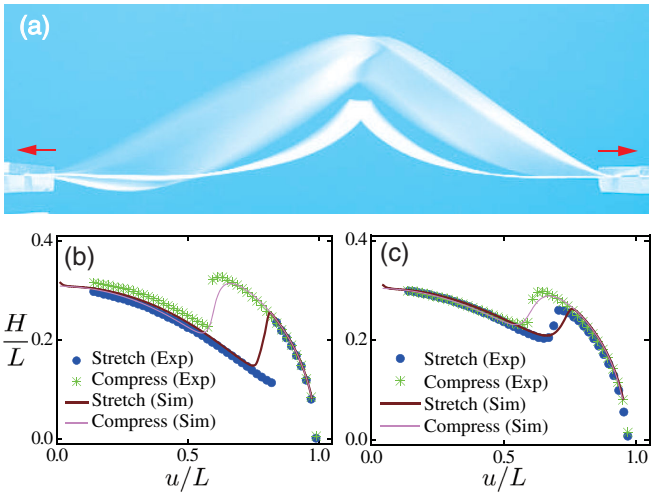

FIG. 3. (a) Superimposed photograph of a stretched looped ribbon during its pop out. (b),(c) Comparison between experiments and simulations. Rescaled height of the ribbon's top, H/L, plotted as a function of u/L in the stretching and compressional processes. Symbols are experimental data (stretching: blue filled circles; compression: green asterisks), and solid lines are numerical simulation data. The parameters used are (b) $(L, b, \delta) = (212, 5, 25)$ and (c) (212,5,45).

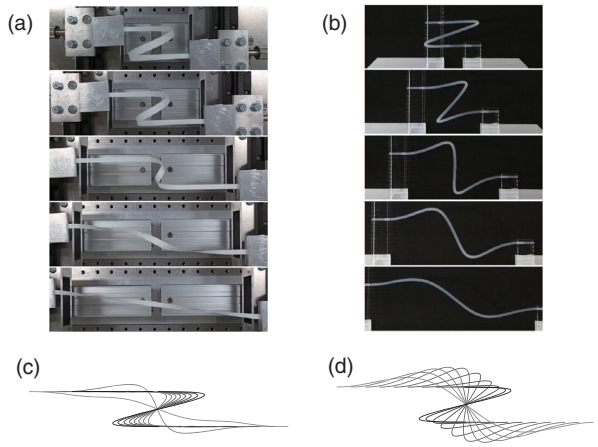

FIG. 4. Comparison of the top views of the loop-opening (i.e., stretching) processes. (a) Paper ribbon with $(L, b, \delta) = (212, 5, 30)$. (b) Silicone rubber rod with circular cross section of diameter 3 mm with $(L, \delta) = (212, 30)$. (a) and (b) are the experimental observations. (c) and (d) represent the centerline configurations during stretch from our numerical simulations for (c) a ribbon and (d) an isotropic rod.

L are scattered, it appears to be generally concave. We will return to the physical interpretation of this later on.

To quantify the nature of the pop out, we measured the height H of a ribbon (see Fig. 1) with (212,5,25) as a function of the extension u [Fig. 3(b)]. This plot manifests the discontinuous increase in H at the pop out. In the inverse (i.e., compressing) process, the discontinuous shape change occurs at a different u, resulting in a large hysteresis during the cycle process, a hallmark of athermal bistable systems.

An insight is obtained by a top-view observation and by comparison with that of a looped slender silicone rubber rod [Figs. 4(a) and 4(b)]. In the earlier stage of the stretching, the loop in the ribbon shrinks keeping its orientation along the stretching axis, while the loop in the rod rotates and gradually opens. These distinctly different behaviors are attributed to the cross-sectional shape, as demonstrated by our numerical simulations explained below [Figs. 4(c) and 4(d)]. For a ribbon, the out-of-plane bending costs much lower energy than the twisting that involves in-plane stretching. This is why the loop initially gets smaller as it is stretched. However, when the loop is tightened and its bending curvature becomes sufficiently large, the cost of stretching becomes comparable to that of bending, leading to the pop-out twist transition. Note that such a process is distinctive to a slender object with a highly anistropic cross section, quantified by b/h. For rods with isotropic cross section, bending and twisting occur simultaneously, which enables the continuous loop opening [Figs. 4(b) and 4(d)]. When the aspect ratio b/L decreases, the anisotropy, i.e., b/h, also decreases, and the loop is likely to open continuously. This explains the behavior of δ_{PT}/L in Fig. 2 for $b/L < 0.04$. Nevertheless, in the limit of the self-contact, the pop out prevails even in a thin metal rod with a circular cross section, as shown in Ref. [23]. We also observed that a silicone rubber ribbon, being elastic up to very large strains, undergoes a twist transition even for $\delta < \delta_{CP}$, accompanying significant in-plane stretch around the loop. This suggests that the crease transition is less likely for more stretchable ribbons. Further investigation on a hyperelastic ribbon is currently under progress and the results will be reported elsewhere [28].

The observed elastic responses are rationalized by our numerical simulations based on the method originally introduced in Ref. [31]. In short, our method relies on the Kirchhoff elastic rod formulation for a narrow ribbon ($L/b \gg 1$), in which a weak stretch is considered in a perturbative way similar to Ref. [29]. In the dynamical simulations, a ribbon centerline is a chain of $N = L/a$ segments of constant length and mass, and the position and velocity of each segment evolve according to Newton's equations of motion with viscous damping terms. Upon rescaling of the equations, all values of the nondimensional parameters are taken from our experiments. The computation thus contains no adjustable parameters, except for the damping parameter. Our numerical results are insensitive to precise values of the damping parameter, as long as the dynamics is underdamped as valid to our experiments.

A direct comparison between the simulations and experiments is shown in Figs. 3(b) and 3(c). The agreement is quantitative in Fig. 3(c) for $\delta = 45$ mm, and is less satisfactory in Fig. 3(b) for $\delta = 25$ mm. The latter is expected, because as δ gets smaller, the in-plane stretch

becomes progressively more significant beyond the validity of our model [32].

To overcome the difficulty manifested for the small δ regime, we now develop a simple scaling argument instead of extending the numerical approach. We argue on the critical loop size R^* at the pop out, focusing on the stretching process. First, we note that an external force applied at the ends scales as $F \sim Db/R^2$, where R is a typical loop size and $D = Eh^3/12(1-\nu^2)$ is a ribbon's bending modulus (E is the Young's modulus and ν is the Poisson ratio) [9]. The external moment that tries to rotate the loop is thus $M_{\rm ext} \sim F\delta \sim Db\delta/R^2$ (see Fig. 5, left). At the pop out, this moment balances with the internal elastic moment $M_{\rm twist}$, which consists of two parts, $M_{\rm twist} = M_{\rm Kirch} + M_{\rm stretch}$. Here, $M_{\rm Kirch} \sim Db\tau$ is the linear Kirchhoff twisting moment (arising from the strain energy over the thickness of the ribbon), while $M_{\rm stretch}$ arises from the in-plane stretch elasticity, where we have introduced the twist per unit length τ that scales as $\tau \sim 1/\delta$ at the pop out. To establish the scaling for $M_{\rm stretch}$, we assume a helicoidal twisting with its Gaussian curvature $-\tau^2$. This induces the in-plane strain $\epsilon \sim -b^2\tau^2$, and the corresponding elastic energy per unit length $E_{\rm stretch} \sim E\epsilon^2 bh \sim Ehb^5\tau^4$, leading to $M_{\rm stretch} \sim Ehb^5\tau^3$. By equating $M_{\rm Kirch}$ and $M_{\rm stretch}$ to examine the relative significance, we conclude that the linear relation $M_{\rm twist} \sim M_{\rm Kirch}$ holds for $\xi \ll \delta$, while the nonlinear response $M_{\rm twist} \sim M_{\rm stretch}$ dominates for $\xi \gg \delta$, where we have defined the characteristic length $\xi \sim b^2/h$. The nondimensional parameter δ/ξ thus measures the relative importance of in-plane stretching over the bending, analogous to the Föpple–von Kármán number for curved shells [33].

For $\xi \ll \delta$, $M_{\rm ext} \sim M_{\rm twist}$ results in the simple scaling relation given by $R^* \sim \delta$. In contrast, for $\xi \gg \delta$, balancing $M_{\rm ext}$ with $M_{\rm stretch}$ yields a different scaling given by $R^* \sim \delta^2/\xi$. Therefore, we conclude

$$R^*/\xi \sim \begin{cases} \delta/\xi & \text{for} \quad \delta/\xi \gg 1 \\ (\delta/\xi)^2 & \text{for} \quad \delta/\xi \ll 1. \end{cases} \tag{2}$$

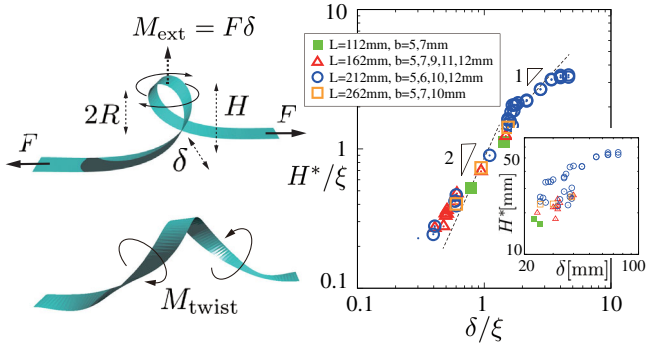

FIG. 5. Left: Schematics on the ribbon's shape and definition of the variables used in the scaling argument. Right: Rescaled plot of the critical ribbon height H^*/ξ vs δ/ξ obtained from our physical experiments for different ribbon width b and length L. Inset is the plot of the same data in the physical units.

To validate the prediction in Eq. (2), the rescaled critical height of the ribbon's top H^*/ξ obtained for varying L, b, and δ in our physical experiments are plotted against the rescaled gap distance δ/ξ in Fig. 5 (the inset is a plot of the same data in the physical units). Note that we have used $\xi = (Ehb^4/720D)^{1/2} \approx 0.12b^2/h$ derived from the perturbation theory [28,29], where $\nu = 0.3$ is assumed.

Note also that we make use of H^* instead of R^* for the comparison in Fig. 5. Considering the difficulty in determining R^* directly from the experimental images, H^* is advantageous because it is comparable to $2R^*$ and is determined precisely from Fig. 3. The data collapse perfectly owing to the rescaling by ξ, and the different slopes cross over at around $\delta/\xi \sim 1$–2, in full agreement with Eq. (2). Not surprisingly, the predicted exponents are less convincing, as H^* may receive an additional contribution from the ribbon's arm, and a weak plastic response might be involved. Nevertheless, Fig. 5 demonstrates that this elastic instability is fully governed by the single characteristic length ξ.

Compiling all the results obtained so far, we propose the following physical scenario. Initially, a ribbon behaves like a developable surface, and the loop progressively gets smaller during the stretching because of its bending anisotropy. In this regime, the overall ribbon shape is well represented by the 1D centerline geometry. As the curvature of the loop becomes even larger, the elastic stress further concentrates around the loop. For $\delta < \delta_{CP}$ given in Eq. (1), the loop geometry undergoes the dimensional crossover from 1D- to 2D-like, leading finally to a crease formation. This marks the breakdown of ribbon's elasticity. In contrast, for $\delta > \delta_{CP}$, there opens an alternative route for a ribbon to avoid such a stress focusing. The ribbon pops out, making use of its 3D configurational degrees of freedom. For this transition, the ribbon has to pay the energetic costs of in-plane stretch, compromising its developability. However, the ribbon responds elastically throughout the regime, which could be described by the existing effective 1D ribbon models.

In summary, by combining experiments and theory, we have investigated the distinct mechanics of a looped ribbon under tension, and demonstrated the central role of the characteristic length $\xi \sim b^2/h$. One may surely notice, however, that papers are not ideal elastic materials [34]; a permanent natural curvature arises due to creeplike deformations [35]. This will significantly affect the unfolding dynamics of a tight loop [36]. It is also important to investigate whether the same physical scenario described here applies to ribbons made from other materials such as glass or metals, as well as nanoscale materials [38,39]. The experimental setup studied here is simple enough, yet raises

a number of interesting open questions, which will thus prolifically generate challenging future subjects.

We acknowledge financial support from KAKENHI (No. 15H03712) from MEXT, Japan and JSPS KAKENHI No. 16H00815: "Synergy of Fluctuation and Structure: Quest for Universal Laws in Non-Equilibrium Systems."

*hwada@fc.ritsumei.ac.jp
†tanaka-yoshimi-vm@ynu.ac.jp

[1] R. Schleif, Annu. Rev. Biochem. **61**, 199 (1992).
[2] I. M. Kulic and H. Schiessel, Phys. Rev. Lett. **92**, 228101 (2004).
[3] X. Y. Kong and Z. L. Wang, Appl. Phys. Lett. **84**, 975 (2004).
[4] J. Hendry, *Wrapping Culture: Politeness, Presentation, and Power in Japan and Other Societies* (Oxford University Press, New York, 1995).
[5] P. Pieranski, S. Kasas, G. Dietler, J. Dubochet, and A. Stasiak, New J. Phys. **3**, 10 (2001).
[6] M. K. Jawed, P. Dieleman, B. Audoly, and P. M. Reis, Phys. Rev. Lett. **115**, 118302 (2015).
[7] T. Yabuta, Bull. JSME **27**, 1821 (1984).
[8] A. Goriely and M. Tabor, Nonlinear Dyn. **21**, 101 (2000).
[9] B. Audoly and Y. Pomeau, *Elasticity and Geometry* (Oxford University Press, New York, 2010).
[10] L. Giomi and L. Mahadevan, Phys. Rev. Lett. **104**, 238104 (2010).
[11] J. Huang, J. Liu, B. Kroll, K. Bertoldi, and D. R. Clarke, Soft Matter **8**, 6291 (2012).
[12] J. Chopin and A. Kudrolli, Phys. Rev. Lett. **111**, 174302 (2013).
[13] J. Chopin, V. Demery, and B. Davidovitch, J. Elast. **119**, 137 (2015).
[14] M. Sadowsky, Sitzungsber. Preuss. Akad. Wiss. Phys. Math. Kl. **22**, 412 (1930).
[15] W. Wunderlich, Monatshefte fur Mathematik **66**, 276 (1962).
[16] E. Efrati, E. Sharon, and R. Kupferman, Phys. Rev. E **83**, 046602 (2011).
[17] M. A. Dias and B. Audoly, in *The Mechanics of Ribbons and Mobius Bands* (Springer The Netherlands, 2016), pp. 49–66.
[18] D. Grossman, E. Sharon, and H. Diamant, Phys. Rev. Lett. **116**, 258105 (2016).
[19] D. A. Kessler and Y. Rabin, Phys. Rev. Lett. **90**, 024301 (2003).
[20] H. Wada and R. R. Netz, Europhys. Lett. **77**, 68001 (2007).
[21] E. L. Starostin and G. H. M. van der Heijden, Phys. Rev. Lett. **101**, 084301 (2008).
[22] E. L. Starostin and G. van der Heijden, J. Mech. Phys. Solids **57**, 959 (2009).
[23] V. Goss, G. van der Heijden, J. Thompson, and S. Neukirch, Exp. Mech. **45**, 101 (2005).
[24] E. Zajac, J. Appl. Mech. **29**, 136 (1962).
[25] I. M. Kulic, H. Mohrbach, R. Thaokar, and H. Schiessel, Phys. Rev. E **75**, 011913 (2007).
[26] F. Lechenault, B. Thiria, and M. Adda-Bedia, Phys. Rev. Lett. **112**, 244301 (2014).
[27] The overall shape of $p(\delta)$ can be well fitted by the error function. The statistical properties of the transitions will be reported in more detail elsewhere [28].
[28] Y. Tanaka and H. Wada (to be published).
[29] R. Ghafouri and R. Bruinsma, Phys. Rev. Lett. **94**, 138101 (2005).
[30] S. Armon, H. Aharoni, M. Moshe, and E. Sharon, Soft Matter **10**, 2733 (2014).
[31] G. Chirico and J. Langowski, Biopolymers **34**, 415 (1994).
[32] Note that the Kirchhoff rod model that entirely ignores in-plane stretch provides less satisfactory agreement with the experiments, even for $\delta = 45$ mm (data not shown), underpinning the usefulness of our perturbative approach.
[33] J. Lidmar, L. Mirny, and D. R. Nelson, Phys. Rev. E **68**, 051910 (2003).
[34] M. Alava and K. Niskanen, Rep. Prog. Phys. **69**, 669 (2006).
[35] M. Mustalahti, J. Rosti, J. Koivisto, and M. Alava, J. Stat. Mech. Theor. Exp. (**2010**) P07019.
[36] Our preliminary simulations including a stress-induced natural curvature in the framework of the morphoelasticity [37] render an excellent quantitative agreement with the experimental data [in Fig. 3(c)] [28].
[37] R. E. Goldstein and A. Goriely, Phys. Rev. E **74**, 010901(R) (2006).
[38] H. Wang and M. Upmanyu, Nanoscale **4**, 3620 (2012).
[39] O. O. Kit, T. Tallinen, L. Mahadevan, J. Timonen, and P. Koskinen, Phys. Rev. B **85**, 085428 (2012).